RSC Advances

PAPER

View Article Online
View Journal | View Issue

Cite this: *RSC Adv.*, 2025, **15**, 11377

Analyzing the effect of isopropylation on regular and high oleic soybean oils: a lubrication behavior perspective†

Piash Bhowmik,[a] Majher I. Sarker,[b] Brajendra K. Sharma,[b] Yachao Wang,[a] Clement Tang[a] and Sougata Roy *[c]

Researchers around the world are focusing on the development of biobased lubricating oils due to the depletion of mineral oil and environmental pollution. Soybean, which is one of the most produced crops globally, has been identified as a potential source for such oil. However, soybean oil has poor thermal and oxidative stability, which needs to be addressed so that soybean oil based lubricants can perform reasonably in relatively high temperature applications. To overcome this, isopropylation based chemical modification was used on both regular soybean oil (RSO) and high oleic soybean oil (HOSO). During this process the carbon–carbon double bonds of fatty acids also get converted to single bonds. To ensure the formation of single bonds, various tests such as GC-MS, NMR, and compact mass spectroscopy (CMS) analyses were performed. The tribological characteristics of the oils were also compared at different temperature conditions. It was observed that the selected chemical modification process was more impactful on RSO from a lubrication perspective, resulting in a 35% reduction in wear volume at room temperature and a 15% reduction at high temperature, compared to only around a 10% reduction for HOSO at both room and high temperatures. Detailed analyses of tribological behavior were conducted by leveraging a suit of microscopy, spectroscopy and interferometry techniques exploring the dominant wear mechanisms in each case.

Received 3rd January 2025
Accepted 24th March 2025

DOI: 10.1039/d5ra00058k

rsc.li/rsc-advances

1. Introduction

The performance of engines and other machinery can be significantly impacted by two major factors – friction and wear. Friction, which is the resistance between two surfaces in motion, is commonly observed at piston rings, bearings, and valve train components in IC engines.[1] Excessive friction can result in energy loss, reduced efficiency, and increased temperatures. However, wear is the gradual material transformation, which can cause critical parts to get damaged, leading to increased clearances, loss of compression, and eventual engine failure. To mitigate these effects, lubricating oil is used to minimize friction and wear, thereby improving the overall performance as well as the lifespan of the machinery. The rapid growth of industries, technological advancements, and urbanization have led to an unprecedented increase in energy demand worldwide. As per estimates provided by Saidur *et al.*,[2] the total global energy consumption is projected to increase by 33.5% by 2030. Such high energy requirements are typically fulfilled by the use of fossil fuels, which in turn necessitates an increased production of petroleum-based products like fuel and lubricants. It is estimated that around 30 to 40 million tons of lubricants are annually used to meet this demand.[3] Petroleum-based lubricating oils are known to be toxic and non-biodegradable, which poses a significant threat to the environment. Their usage can result in detrimental ecological impacts.[4,5] It's worth noting that most of the lubricants that enter the environment, specifically more than 95% of them, are derived from petroleum and can cause significant harm to the environment.[6]

There is a growing global focus on minimizing the reliance on petroleum-based products observing their negative environmental effects. One of the main challenges with such products is their non-renewable nature, alongside concerns on toxicity and biodegradability. As a result, environmental regulations are becoming increasingly strict, driven by concerns about limited fossil fuel reserves and heightened environmental risks.[7] In response, researchers are taking measures aimed at slowing down environmental degradation and reducing our reliance on non-renewable resources. These measures include the development of green energy systems and the exploration of

[a]*Department of Mechanical Engineering, University of North Dakota, Grand Forks, ND, USA*

[b]*Sustainable Biofuels and Coproducts Research, USDA-ARS-NEA-ERRC, Wyndmoor, PA, USA*

[c]*Department of Mechanical Engineering, Iowa State University, Ames, IA, USA. E-mail: sroy@iastate.edu*

† Electronic supplementary information (ESI) available. See DOI: https://doi.org/10.1039/d5ra00058k

renewable resources as alternative options to mineral-based products.[8,9] The demand for biobased lubricants is on the rise, and with it, the market for these eco-friendly products is steadily growing. To meet this demand, researchers are exploring different types of biobased oils such as canola oil,[10–14] soybean oil,[7–9,15] coffee bean oil,[16,17] avocado oil,[10] sunflower oil,[18–20] palm oil,[21–23] jatropha oil,[24,25] rapeseed oil,[24] coconut oil,[26–28] waste cooking oil,[29] fish oil,[30,31] animal fats[32,33] and algal oil,[34,35] as the base oils for these lubricating oils. The major benefits of using biobased lubricants are nontoxicity and biodegradability. Bio-based oils mainly contain triglycerides, which microorganisms can easily break down. This makes them more biodegradable than synthetic oils, which have complex, resistant structures.[36] Although renewable oils are typically biodegradable, their degradability depends on changes in the chemical structure of the base oil during use. Modifications such as oxidation, polymerization, or the addition of resistant chemical groups can reduce their ability to break down naturally.[37] Additionally, these oils present low volatility and limited range of viscosity change with the alteration of temperature since they are composed of triglycerides which have high molecular weight.[12]

Despite the numerous advantages that bio-based lubricants offer, their widespread adoption is hindered by major challenges associated with their performance. Major limitations of these oils as lubricants are their poor cold flow properties and high affinity to oxidation, which can result in degradation and polymerization. In unsaturated fatty acids (*e.g.* oleic acid, and linoleic acid), double bonds can get easily oxidized and the polyunsaturated fatty acids are even more prone because of the bis-allylic protons located between two double bonds. The oxidation process of lubricants occurs in three stages: initiation, propagation, and termination. First, lubricant components react and produce free radicals, which are highly reactive. In propagation stage, free radicals and catalysts interact to produce more free radicals and oxygenated compounds. The oxidation process concludes in the termination stage, which can have either a positive or negative outcome. However, this challenge can be effectively addressed through chemical modifications or by incorporating suitable additives to enhance their performance. Shrivastava *et al.*[38] developed a new technique for producing biodiesel and biolubricants from soybean oil by utilizing Zn Al hydrotalcite as a heterogeneous catalyst. They carried out a double transesterification of soybean oil with methanol and trimethylolpropane (TMP) to generate fatty acid alkyl esters and trimethylolpropane fatty acid triester (TFATE), respectively. Furthermore, they evaluated the tribological properties of the newly developed bio-lubricant, which exhibited the lowest coefficient of friction. Hwang *et al.*[39] created synthetic lubricant base stocks by combining Guerbet alcohols with epoxidized soybean oil (ESO). They employed a ring-opening reaction, followed by transesterification to achieve their desired end products. By acetylating the ring-opened product, they were able to decrease viscosities while increasing the viscosity indices of the final products. Another chemical modification process is hydrogenation, in which hydrogen gas is added to a substance, such as vegetable oil, to convert unsaturated oils into saturated oils. In a recent study, Fathurrahman *et al.*[40] analyzed the effects of combining palm oil biodiesel (POB) with commercial petroleum-based diesel fuel (DF) and hydrogenated vegetable oil (HVO) at different blend points. They discovered that adding POB to the diesel fuel blends improved their lubricating properties, leading to a decreased friction coefficient and a lower wear rate. Sarker *et al.*[32,33,41] investigated the isopropylation method on regular lard, beef tallow, and chicken fat. They chemically modified the triglyceride structures by introducing isopropyl groups using ethylaluminum sesquichloride ($Et_3Al_2Cl_3$). The results showed that the modified beef tallow and lard exhibited significant improvements in low-temperature properties, oxidative stability, density, and kinematic viscosity. The chicken fat which was modified chemically displayed higher density and enhanced oxidation stability, with improved kinematic viscosity as compared to regular chicken fat and high oleic sunflower oil (HOSuO). Bhowmik *et al.*[13] conducted a study on high oleic soybean oil (HOSO) using a similar approached and revealed its effect on tribological behavior. The chemical modification process utilized resulted in a 10% increase in wear resistance at both room and 100 °C temperatures compared to regular HOSO. This also demonstrated improved oxidation stability and decreased pour point characteristics in the chemically modified HOSO.

In this study, the tribological performance and physico-chemical characteristics of regular soybean oil (RSO) and HOSO were compared after undergoing a chemical modification process using isopropyl bromide. This process, known as isopropylation, introduced branching at the double bond site and converted double bonds to single bonds to enhance oxidation resistance, as unsaturated fatty acids are prone to oxidation. Additionally, the oil's cold flow properties improve as the flexibility of single bonds reduces molecular packing.[13] To enable the addition of isopropyl group to the double bonds, a Lewis acid catalyst, such as ethylaluminum sesquichloride ($Et_3Al_2Cl_3$), was employed. The process started with the interaction of the catalyst with isopropyl bromide, resulting in the formation of a carbocation intermediate. This intermediate was formed when the catalyst attacks the isopropyl bromide molecule. The subsequent step involved the reaction of the carbocation intermediate with the electron-rich double bond of the fatty acid, leading to the creation of carbon–carbon single bonds. The major findings from this investigation can serve as a guideline for next generation chemists and engineers to select proper oil type and chemical modification process which can meet lubricant properties and its friction and wear behavior.

2. Methodology

2.1 Materials

The RSO and HOSO were purchased from CHS Inc., located in Minnesota, USA. Meanwhile, BRSO and BHOSO were modified from RSO and HOSO, respectively as described later. The fatty acid composition of the oils was determined using Gas Chromatography-Mass Spectroscopy (GC-MS). The material selection for ball and flat samples of tribo-testing was inspired

by hybrid bearing materials with silicon nitride (Si_3N_4) balls and AISI 52100 flats serving as counterparts. The most common bearing material is AISI 52100 steel due to its favorable combination of properties including high hardness, wear resistance, toughness, availability, and cost-effectiveness.[42] Hybrid bearings use ceramic balls to offer benefits like faster speeds, more stiffness, less friction, and reduced heat.[43] These bearings, which combine ceramic balls with steel counterparts, are frequently utilized in electric vehicles. The motor rotation generates shaft currents that can cause electrochemical corrosion and result in surface damage to the bearings, which is the primary reason behind selection of hybrid bearings.[44] The use of ceramic balls helps to prevent such challenges by creating an electrical insulation and providing enhanced durability against wear.[45,46]

2.2 Synthesis of branched regular soybean oil (BRSO)

The synthesis of isopropyl branched RSO (BRSO) from RSO is illustrated in Fig. 1. A round-bottom flask with a septum was used to dissolve 70 g (approximately 0.079 mol) of RSO in methylene chloride, followed by cooling the flask in an ice bath and then flushing it with argon gas. After a slow addition of 88.5 g (~0.36 mole) of ethylaluminum sesquichloride ($Et_3Al_2Cl_3$) over 30 minutes using a dropping funnel, 44.0 g (~0.36 mole) of isopropyl bromide was then added. After adding the isopropyl bromide, the mixture was stirred in an ice bath for a duration of one hour and then allowed to stir overnight at room temperature in an inert argon environment. Thin Layer Chromatography (TLC) was used to verify the reaction's completion. Ethyl acetate (100 mL) was mixed with the mixture and then 10% hydrochloric acid (HCl) was gradually added in an amount of 10 mL until distinct aqueous and organic layers were observed. Subsequently, the organic layer underwent three washes with water (150 mL) and one wash with brine solution (150 mL). The remaining water in the organic phase was removed by adding anhydrous sodium sulfate, followed by evaporating the ethyl acetate using a rotary evaporator, resulting in a 92% yield relative to the initial amount of RSO. The modification of BHOSO from HOSO was carried out following the same protocol.

2.3 Nuclear magnetic resonance (NMR)

A 14 Tesla NMR (made by Agilent Technologies, Santa Clara, CA) was used to analyze the samples. The spectrometer utilizes a 5 mm One NMR probe for analysis. All samples were dissolved in deuterated chloroform sourced from Cambridge Isotope Laboratories in Andover, MA, and then analyzed at a temperature of 25 °C. The ^1H spectra were acquired using a 2 second relaxation delay and a 2.28 second acquisition time with a 45° pulse angle. The spectral width was 12 parts per million (ppm). For the ^{13}C spectra, a 45° pulse angle, 2 second relaxation delay, and 0.87 second acquisition time, averaging 1000 transients, were employed. The spectral widths of these spectra were 253 ppm. The spectra were processed with SpinWorks4 software (v4.2.10), which was developed by Kirk Marat at the University of Manitoba, Canada.

2.4 Gas chromatography-mass spectroscopy (GC-MS)

To determine the fatty acid composition of the starting materials (RSO) and products (BRSO), a Gas Chromatograph (model 8890N) from Agilent Technologies was used. This Gas Chromatograph was equipped with an Agilent model 5977N mass selective (MS) detector. Additionally, a Supelco SP-2380 column (30 m length, 0.25 mm diameter, 0.2 μm film thickness) was employed for the analysis. For the GC-MS analysis, RSO and BRSO were first transesterified to produce fatty acid methyl esters (FAME). About 100 mg of sample was placed in 20 mL reaction vials, to which 15 mL of 2% sulfuric acid (H_2SO_4) in methanol was added. The vials were then sealed and stirred at 80 °C for 2 hours. After the reaction, the mixture was cooled to room temperature, and the methanol evaporated under vacuum. The desired FAME was then extracted from the mixture using an ethyl acetate extraction process. The crude product underwent three washes with 15 mL water to eliminate any leftover glycerol and acid catalyst from the FAME. Subsequently, the ethyl acetate extract containing the fatty acid methyl esters (FAME) was further treated with a 5 mL brine solution wash. Na_2SO_4 (anhydrous sodium sulfate) was then used to dry the extract. The samples were prepared for GC-MS analysis by diluting 5 μL of the ethyl acetate extract with 1 mL of ethyl acetate before putting it into the machine. The column was first heated to 70 °C and maintained at this temperature for 2 minutes. The column temperature gradually increased to 250 °C at a rate of 20 °C per minute and then maintained at that temperature for 10 minutes. Helium gas was used as carrier gas, flowing at a rate of 1.5 mL per minute with a split ratio of 50 : 1. The injector was set to 230 °C, and the detector was held at 280 °C.

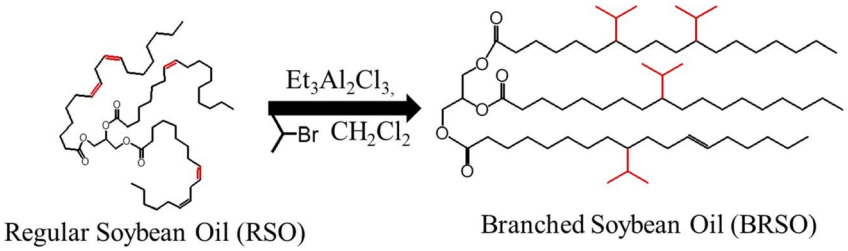

Fig. 1 Synthesis of BRSO *via* isopropylation of RSO.

2.5 Compact mass spectroscopy (CMS)

Advion (Ithaca, New York) Expression Compact Mass Spectrometer (CMS) was used to determine molecular weight of RSO and BRSO and their fragments. In CMS, a single quadrupole mass analyzer with an atmospheric pressure interface is built-in, which provides both electrospray ionization (ESI) and atmospheric pressure chemical ionization (APCI) capabilities with positive and negative polarity switching within a single analysis. The CMS provides mass measurements over a mass range of 0–2000 *m*/*z*. The Expression CMS allows for rapid compound confirmation and identification in normal and reverse phase chromatographic applications compatible with ultra performance liquid chromatography and supercritical fluid chromatography.

For this study, APCI ion source was used to achieve data acquisition, where capillary temperature was set at 300 °C and capillary voltage at 80 volts. Source gas was nitrogen at temperature 350 °C and pressure at 4.8×10^{-3} mbar. The mobile phase solvent used was HPLC grade methanol from Sigma Aldrich at a flow rate of 0.5 mL min^{-1}. The range for acquisition measured mass was set from 250–2000 *m*/*z* and scan time captured at 1000 (ms) with a scan speed of 1750 (*m*/*z* per sec). The volume of sample injected into the APCI source for analysis was 20 μl at a concentration of ~10–50 ppm.

2.6 Pressure differential scanning calorimetry (PDSC)

The samples' DSC thermograms were obtained using a TA Instruments Q20 instrument from New Castle, DE, USA, following a specific experimental protocol. Around 1.5–2.0 mg of each specimen was measured and sealed in an aluminum pan with lids equipped with small holes to ensure proper interaction with dry air, a reactant. Regulated gas diffusion through a small opening enabled the oil sample to saturate with air while preventing its evaporation. Maintaining the thickness of the oil film (<1 mm) in the pan was essential to facilitate effective oil–air interaction, thus preventing any discrepancies in results due to limitations in gas diffusion. The PDSC temperature calibration utilized indium metal's melting temperature of 156.6 °C as a reference, with a heating rate of 10 °C per minute. After loading the sample pan into the PDSC cell, it was sealed and pressurized with dry air to 200 psi (1378.95 kPa). The temperature of the cell steadily increased by 10 °C every minute, starting from ambient temperature and reaching 300 °C. During this process, data was collected to analyze the sample's properties. The software provided heat flow (W g^{-1}) *versus* temperature plots that were used to determine the oxidation Onset Temperature (OT, °C) and oxidation Peak Temperature (PT, °C). To obtain accurate results, each sample underwent three distinct tests. The results were reported using the mean values, rounded to the nearest decimal place.

2.7 Viscosity, density, and viscosity index analysis

The viscosity and densities of biobased oils at 40 °C and 100 °C were determined using an Anton Paar GmbH SVM3001/G2 viscometer equipped with an Xsample 530 automatic sample changer. The testing was conducted in compliance with ASTM D7042 [47] and ASTM D4052.[48] Each sample was transferred into a vial and then these vials were put into the carousel of the automated sample changer. The instrument autonomously calculated the kinematic viscosity readings using dynamic viscosity and density measurements. According to ASTM D2270 [49] guidelines, the viscosity index (VI) of biobased oils was automatically derived from the kinematic viscosity data.

2.8 Cloud point (CP)

To assess the cloud point, guidelines were followed provided by ASTM D5773 [50] using an automated instrument called Phase Technology PSA-70x. Before testing, the sample oils were stored at a consistent temperature of 22 ± 1 °C in the laboratory. The instrument was equipped with a sealed chamber that had a reflective bottom surface. A precise volume of 0.150 ± 0.005 mL of the sample was placed inside the chamber, which was then vacuumed to remove any surrounding moisture. The samples underwent gradual cooling at a consistent rate of 1.5 ± 0.1 °C every minute. During the cooling process, an internal light source illuminated the sample from an angle, while an optical detector positioned directly above continuously monitored its status. As long as the specimen remained in its fluid form, the light penetrated through it, reflecting off the chamber's bottom. Upon the initiation of crystal formation during cooling, the scattered light redirected some of its rays towards the optical sensor positioned above the specimen. When the scattered light was directed onto the optical sensor, this temperature could be used to determine the cloud point, where crystals typically form, across a range from −60 °C to 49 °C.

2.9 Pour point (PP)

Following the determination of the cloud point, the analysis to measure the pour point was conducted according to D5949.[51] The sample was subjected to a burst of dry air, which led to a visible alteration in optical scattering detected by the optical sensor. The cooling rate of the sample was maintained at a steady 1.5 °C per minute, with bursts of dry air introduced intermittently at 3 °C intervals. Upon freezing, no alteration in the optical response of the sample was observed. The pour point was determined by identifying the temperature at which no further optical shift was observed in response to the dry air. For example, if the optical reading remained unchanged at −27 °C when the dry air was introduced, the pour point would be recorded as −24 °C. This method accurately identified the pour point over temperatures ranging from −57 °C to 51 °C.

2.10 Experimental setup for tribology tests

The Rtec MFT2000 (Make: Rtec Instruments, USA), was used to analyze the tribological properties of vegetable oils. The diagram of the tribometer is represented in Fig. 2a. To minimize the use of lubricating oil, a new sample holder was designed and developed, as shown in Fig. 2b, requiring only 8 mL of oil for each test. Considering the resources required for chemical modification, the ability to conduct tribological tests systematically using a lower amount of lubricant was helpful in running multiple repeat experiments in each case. Silicon

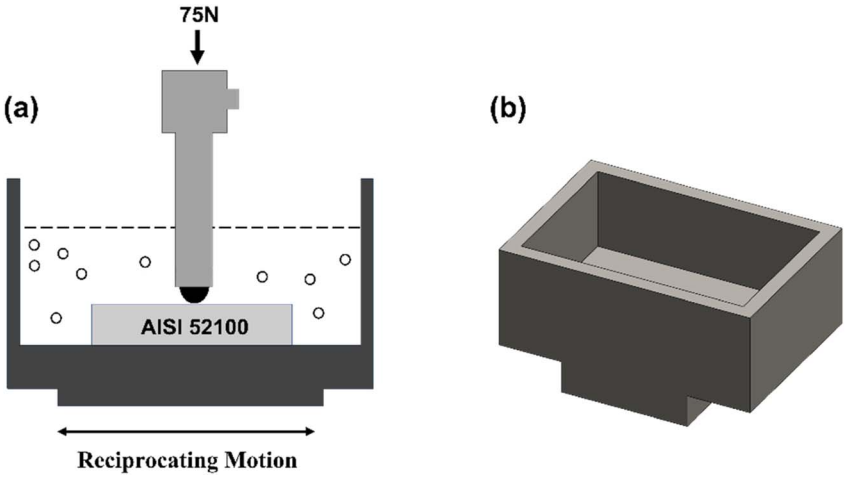

Fig. 2 (a) Schematic representation of the tribological analysis setup. (b) Modified sample holder.

Table 1 Operating test parameters considered during the experiments

Test parameters	Value
Load applied (N)	75
Velocity (m s^{-1})	0.1
Track length (mm)	10
Temperature (°C)	25 & 100
Duration (s)	5040
Total distance (m)	500
Hertzian contact pressure (GPa)	2.7

nitride (Si_3N_4) balls with a diameter of 6 mm were utilized as the counterpart, and the flat surface was made of AISI 52100 steel. The baseline surface roughness of the flat samples was below 0.1 μm, as captured by a white light interferometer (Make: KLA Instruments, USA). The testing conditions considered for the tribo-tests are depicted in Table 1. To compare the tribological behavior of chemically modified regular soybean oil, the tribo-test conditions were kept constant (Table 1) as compared to our previous effort.[13] In electric vehicles (EVs), components such as gears and bearings experience higher loads and stresses due to the instant torque generated by electric motors.[52] To replicate these demanding conditions, tribological tests are conducted using higher Hertzian pressures and increased loads to evaluate the lubricant's ability to withstand elevated contact stresses. Additionally, moderate sliding velocity (5 Hz with 0.1 m s^{-1}) was selected to reflect the high-speed operation of EV transmissions.[53] Considering high temperature generation in gearbox, the tests were conducted both at room temperature and 100 °C levels. The experiments were repeated three times under each test condition to ensure the reliability of the captured findings. Following the experiments, the volume and depth of each wear track were measured using a white light interferometer. The analysis of wear mechanisms was conducted by a Quanta FEG 650 Scanning Electron Microscope (SEM) (Make: FEI Inc.,USA) attached with a Bruker Nano XFlash SUE 6 Energy Dispersive X-Ray Spectroscopy (EDS) system (manufactured by Bruker Inc. in the USA).

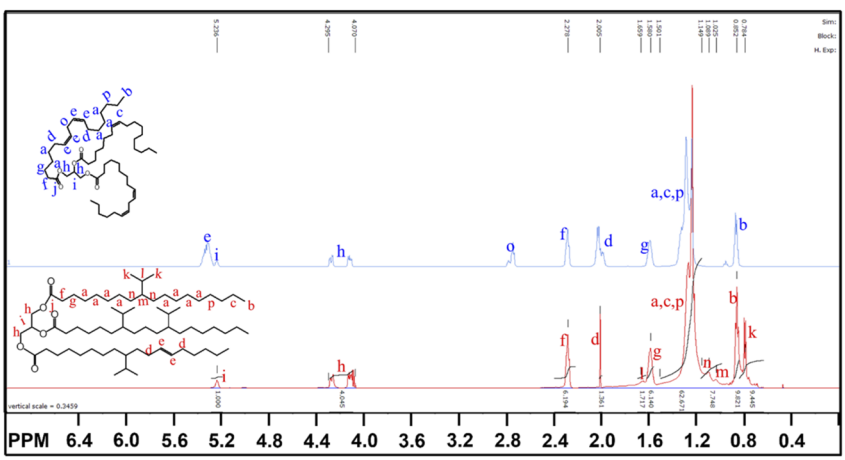

Fig. 3 Comparison between the ^{1}H NMR of RSO (top blue line) and BRSO (bottom red line). Spectral peaks are assigned with their corresponding protons in letters.

2.11 Experimental testing of the lubricants

2.11.1. NMR analysis. The proton and carbon NMR investigations definitively detected the existence of isopropyl (i-Pr) groups in the BRSO triglyceride molecule, as shown in Fig. 3 and S1† (bottom line).

The peak at 0.78 ppm in Fig. 3 (bottom red line) represents the $-CH_3$ protons of the isopropyl (i-Pr) groups in BRSO. These protons are not present in the RSO proton spectra (Fig. 3, top blue line). The –CH– from the isopropyl (i-Pr) group was seen at a chemical shift of 1.66 ppm, exhibiting a multiplet signal. The signals at 1.03 and 1.09 ppm corresponded to the –CH–i-Pr moiety and its adjacent $-CH_2$ protons, respectively. The number of isopropyl (i-Pr) groups in a BRSO molecule was determined from the peak area integration of the $-CH_3$ protons to be 9.45/6 = 1.6 i-Pr groups/triglyceride. The –CH– proton of the i-Pr group similarly exhibited a comparable value of 1.7. In a previous study,[13] isopropylation of HOSO incorporated 2.32 i-Pr groups per branched high oleic soybean oil (BHOSO) molecule. The RSO spectra displayed peaks corresponding to the allylic (2.0 ppm) and vinylic protons (5.33 ppm). Unlike HOSO, RSOY spectrum also showed bis allylic (2.75 ppm) protons indicating polyunsaturated fatty acid chains present in RSO. However, only the allylic protons were observable in the BRSO spectrum, suggesting that only a small number of C=C bonds remained unreacted. From the allylic peak area integration of BRSO, it was calculated that 1.36/4 = 0.34 C=C were present per triglyceride molecule. However, the number of C=C present per triglyceride molecule in RSO was 4.7, which was calculated from the peak area integration for vinylic protons (5.33 ppm) of RSO (peak area integration of RSO is not shown in Fig. 3). Therefore, only 0.34/4.7 × 100 = 7.2% C=C remained unsaturated. The spectra of both BRSO and RSO (Fig. 3) exhibited three prominent peaks at 4.12, 4.26, and 5.23 ppm. These peaks correspond to the protons of the glycerol backbone, indicating that the backbone remained intact in BRSO following the alkylation reaction.

The ^{13}C spectrum of the BRSO (Fig. S1,† represented by the bottom red line) exhibited peaks at 19.0 ppm, 27.6 ppm, and 43.5 ppm, which can be attributed to the carbon atoms of the isopropyl group. The prominent peaks at 62.0 and 68.8 ppm observed in both RSO and BRSO spectra corresponded to the carbon atoms of the glycerol backbone. The peaks at 172.9 ppm corresponded to the carbonyl carbons of BRSO.

2.11.2. GC-MS analysis. GC-MS data shows FAMEs from RSO (Fig. 4, red line) contain 10.65% methyl (Me) palmitate ($C_{17}H_{34}O_2$), 3.93% Me-stearate ($C_{19}H_{38}O_2$), 20.71% Me-oleate ($C_{19}H_{36}O_2$), 57.94% Me-linoleate ($C_{19}H_{34}O_2$) and 6.78% Me-linolenate ($C_{19}H_{32}O_2$). As a result of chemical modification, most of the unsaturated acid chains of RSO were branched with isopropyl groups to form i-Pr branched methyl stearate ($C_{22}H_{44}O_2$, MW 340). The relative composition of monomeric FAMEs of synthesized BRSO was determined by the GC-MS analysis (Fig. 4, blue line) that included 29.4% of Me-palmitate, 9.2% Me-stearate, 44.0% i-Pr branched Me-stearate, 2.9% i-Pr branched Me-oleate and 14.3% Me-stearate containing two i-Pr branches. The peak representing i-Pr branched Me-stearate ([M+] = 340 *m*/*z*) appeared at 10.8 min retention time, which was mainly produced from the unsaturated fatty acid chains of RSO during chemical modification. The relative percentage of i-Pr branched Me-stearate in BRSO and BHOSO varies significantly as it was calculated 86.3% in BHOSO.[13]

However, A separate GC analysis of BRSO was carried out using DB-5 column (spectrum is not included) to determine the relative composition of oligomers. It was calculated that BRSO contains 36.3% of oligomers, 47.9% i-Pr branched monomeric FAMEs, 5.4% Me-stearate and 10.2% Me-palmitate.

2.11.3. CMS analysis. The CMS analytical spectra of the of RSO and the synthesized BRSO using an APCI ion source are illustrated in Fig. 5. RSO was found to be broken up into three main ions at 880, 856, and 601.6 *m*/*z*, which are represented by the whole molecular ions with different compositions (*m*/*z*: 880 and 856) and diester (601.6 *m*/*z*), respectively shown in Fig. 5A. In Fig. 5B, BRSO was observed to be broken into different

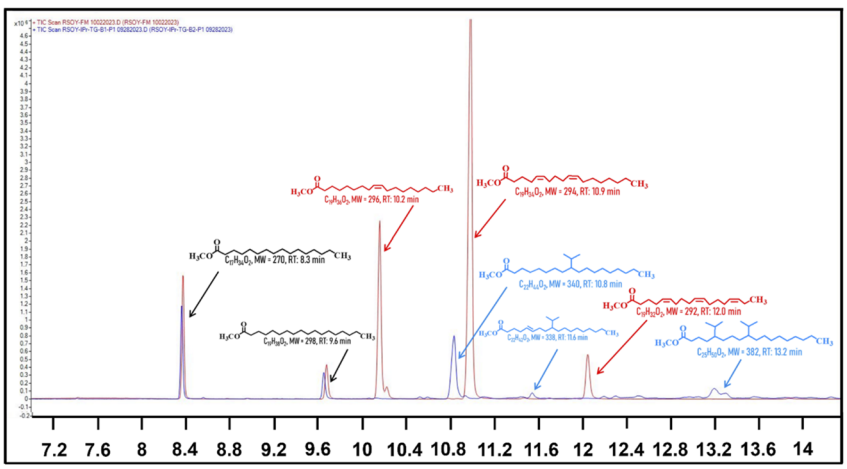

Fig. 4 GC-MS-total ion count *vs.* retention time for FAMEs of RSO (red line) and BRSO (blue line). The peaks are annotated with the FAME chemical formula.

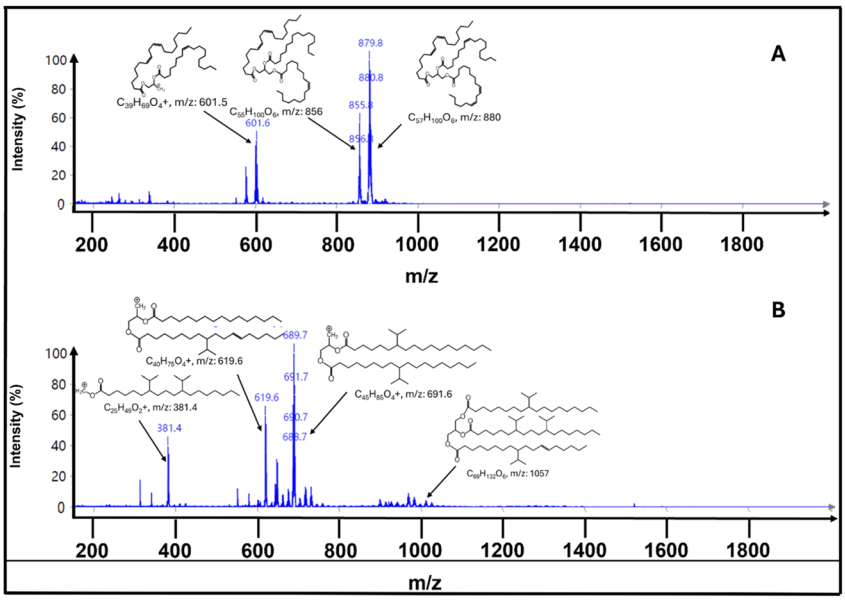

Fig. 5 CMS analysis of (A) RSO; (B) BRSO with their fragmented ions.

fragmented ions, where $m/z = 1057$ represented the whole modified triglyceride ion with multiple branches on fatty acid chains. The fragments, $m/z = 691.6$ and 619.6 represented two dimers with different compositions. One monomeric fragment attaching two i-Pr branches is also shown in Fig. 5B. This data supports the integrity of the chemical structure of BRSO.

2.12 Physico-chemical properties of the sample oils

2.12.1. Density. Density changes due to the introduction of branching in RSO were analyzed at temperatures of 40 °C and 100 °C, outlined in Table 3. The addition of the isopropyl group to RSO resulted in a marginal increase in density at both conditions. For instance, at lower temperature (40 °C), while RSO exhibited a density of 0.9066 g cm^{-3}, BRSO displayed a density of 0.9242 g cm^{-3}. The density rose, likely as a result of the higher molecular weight of BRSO due to the inclusion of i-Pr groups. Additionally, the reduction of *cis*-unsaturation caused the chains in BRSO to become more tightly packed, resulting in increased density. Density decreased with the temperature.[54] The reason for the lower density of the BHOSO is discussed in earlier work.[13]

2.12.2. Kinematic viscosity and viscosity index. Kinematic viscosity quantifies how much resistance a fluid offers to flow due to gravity. Viscosity index (VI) is the fluid's thickness that changes with temperature, with a higher VI indicating stable viscosity across a wide temperature span. The kinematic viscosity and VI are presented in Table 3. At 40 °C, BRSO showed a kinematic viscosity approximately 42 times greater than RSO, while BHOSO exhibited a viscosity about 4 times higher than HOSO at the same temperature. The kinematic viscosity of all the oils decreased as the temperature increased. Viscosity has an inverse relationship with temperature and follows an exponential trend, decreasing more rapidly as temperature rises.[54] At higher temperatures, the modified oils still had higher kinematic viscosity than regular oils, but the difference was not as large as 40 °C. The higher viscosity of the modified oils compared to regular oils was due to the existence of an alkyl branch. This structural feature likely hinders the flow of molecules, leading to an increased kinematic viscosity.[32] Another factor contributing to the higher viscosity of BRSO could be the presence of oligomers.[55] Methyl oleate from RSO had a molecular weight of 296, while i-Pr branched methyl stearate from BRSO had a molecular weight of 340. Previous observations indicate that an increase in molecular weight of a lubricant leads to higher viscosity. Another study found that the viscosity of a substance decreased as the number of double bonds increased.[56] The VI of BRSO (VI: 210.8) was slightly lower than the RSO (VI: 228.4), as shown in Table 3.

2.12.3. Oxidation stability. The oxidation stability of the oils was analyzed using PDSC, and Table 3 presents the temperatures corresponding to the onset oxidation (OT) and peak oxidation (PT). A substance with a higher OT and PT value is more resistant to oxidation. BRSO demonstrated higher PT and OT values compared to RSO. The level of unsaturation impacts the oxidation stability of oils. Fatty acids that are more unsaturated are less stable and more prone to oxidation.[57] BRSO exhibited greater oxidative stability compared to RSO as a result of fewer unsaturated bonds in the fatty acid components of the triglycerides present in BRSO, as confirmed by NMR also. For BRSO, there was an observed increase of 11.4% in OT and 14.6% in PT. However, BHOSO showed no enhancement in OT, with a minimal rise of 1.3% in PT only. These findings suggest that the modification significantly enhances the oxidative stability of RSO more than that of HOSO. The improvement in RSO can be attributed to its composition, which includes around 65% polyunsaturated fatty acids. In contrast, HOSO mostly contains monounsaturated fatty acids. These double bonds are converted into single bonds. Improvements in oxidation stability

contribute to enhanced wear resistance, which will be discussed in a later section.

2.12.4. Cloud point and pour point. The cloud point (CP) is when oil starts to develop a cloudy appearance as it cools. On the other hand, the pour point (PP) is the temperature at which the oil no longer flows. The modified oils had a lower CP than the raw oils as shown in Table 3. These findings suggest that the branching of the fatty acid tail group improved the cold flow properties. With the introduction of branching to the oil, it was possible to reduce its CP by preventing close packing at the time of cooling.[27] For BRSO, the CP decreased significantly from −8.1 °C to −19.1 °C, whereas for BHOSO, it changed from −10.9 °C to −14.5 °C. The improvement in BRSO is notably greater. The significant improvement in BRSO's cloud point enhanced its performance in colder temperatures, ensuring effective operation without solidification. Both BHOSO and BRSO share a similar pour point, with both exhibiting higher values compared to RSO and HOSO, respectively. This could be due to the *trans*-saturated chains in BRSO, which can be stacked more easily than the *cis*-unsaturated chains present in RSO, offering a kink bend that prevents the fatty acids from packing tightly.[54,55] Oils with higher unsaturated fatty acid content typically have lower pour points.[27]

3. Result and discussion

3.1 A comparative analyses of frictional behavior

Reciprocating friction and wear tests were conducted to investigate the effects of chemical modification on RSO and HOSO on frictional behavior under different lubricant cases at room temperature (Fig. 6a) and 100 °C (Fig. 6b) test conditions. The coefficient of friction (COF) of HOSO was found to be the lowest in both temperature conditions. This can be attributed to the presence of tocopherol,[58] which acts as an antioxidant and inhibits the formation of free radicals.[59] The modified version of HOSO (BHOSO) showed a significant increase in friction value by 22%. RSO exhibited a higher friction value than HOSO, while BRSO had the highest COF, showing a 30.4% increase in room temperature. On the other hand, the COF of all samples decreased at 100 °C temperature (Fig. 6b). The decreased friction value can be attributed to the higher mobility of the lubricant at high temperature caused by a decrease in viscosity.[60–62] This finding is consistent with the observation of reduced friction values by Wang *et al.*[63] using IL additives. At high temperatures, the viscosity of IL decreases, enhancing its mobility and spreadability on the DLC film. This reduction in viscosity allows IL to interact more effectively with the DLC film, forming a stable lubricating layer that significantly reduces friction. Zhang *et al.*[64] studied the elastohydrodynamic (EHD) friction properties of various base fluids under mixed sliding-rolling conditions at different temperatures and pressures and found that the COF values decreased with temperature.[64] On the other hand, at high temperature BRSO displayed the highest coefficient of friction, which is consistent with the findings at room temperature. However, the increase in COF at high temperatures was smaller compared to room temperature, with BHOSO rising by 17% and BRSO by 6%.This indicates that BRSO performed better from frictional viewpoint at high temperature compared to room temperature. The higher coefficient of friction (COF) value observed for the modified oils (BHOSO, BRSO) can be attributed to the branching of carbons,[64] as well as the irregular shape, as reported by Hentschel Bayer *et al.*[65] Additionally, a correlation between COF and viscosity was observed. BRSO, with the highest viscosity, exhibited the highest COF, while BHOSO, which had the second-highest viscosity, also showed the second-highest COF. Furthermore, HOSO and RSO demonstrated similar COF values, which can be explained by their nearly identical viscosities. Furthermore, correlation between COF and molecular structure, explains the increased COF value.[66,67] There was no major fluctuation observed in the COF signals for room temperature in all lubricants unlike the

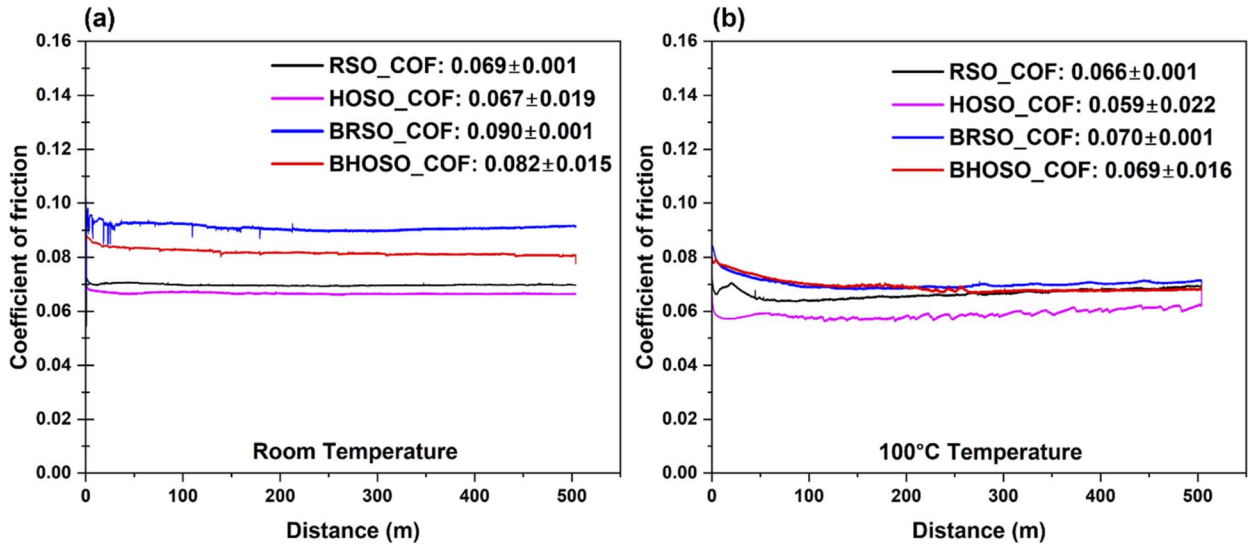

Fig. 6 Coefficient of friction trends of oils (a) room temperature (b) 100 °C temperature.

100 °C operating condition for RSO and HOSO. On the contrary, no significant variations were captured for the modified oils (BRSO and BHOSO), which was likely due to the development of a stable tribofilm caused by saturated fatty acids.[18]

3.2 Wear volume analysis

Fig. 7 demonstrates the wear resistance behavior of regular and chemically modified soybean oil types at room (Fig. 7a) and high (Fig. 7b) temperatures. At room temperature, BRSO exhibited a significant reduction in wear volume from 85×10^6 μm^3 to 55×10^6 μm^3, which represents a 35% decrease, while BHOSO could provide 10.5% reduction in wear volume as compared HOSO. In contrast, at 100 °C, BRSO showed a 15.7% reduction in wear volume, while BHOSO exhibited a 10.5% reduction. These results indicate that the chemical modification of RSO provided better wear resistance than that of HOSO at both temperature levels. This can be attributed to higher percentage of palmitic acid and the presence of oligomer in BRSO (Table 2).

The wear resistance decreased significantly at 100 °C temperature due to a synergistic effect of thermal softening of test material and reduced lubricant viscosity resulting in less surface protection at higher temperature. Attia *et al.*[62] investigated the influence of the operating temperature on the characteristics of soybean oil. They reported significant changes in the viscosity index and thermal stability of these oils due to the temperature variation. If the viscosity of a lubricant is too low, it will be thin and flow easily, potentially leading to insufficient film thickness and increased wear rates due to metal-to-metal contact. Conversely, if the viscosity is too high, the lubricant will be thick, causing flow resistance.

The major difference in wear resistance due to chemical modification for both RSO and HOSO using two-dimensional wear depth profiles for both test temperatures is presented in Fig. 8. At room temperature, the wear depth for all the samples was significantly lower than the wear depth profiles at 100 °C, which is consistent with captured wear volume results at both temperatures. Saturated fatty acids lead to the development of a stable tribofilm, which can be correlated with the reduction in wear depths and volumes[18] observed in this study. However, BRSO had a significantly lower wear track depth and width (Fig. 8) than BHOSO suggesting higher wear resistance of BRSO as compared to BHOSO. This could also be attributed to the higher viscosity of BRSO compared to BHOSO. Due to the superior wear resistance of ceramics compared to metals, the wear volumes observed in balls were significantly lower than those captured in flat samples and hence was not considered in this investigation.

3.3 Wear mechanism analysis

The secondary electron micrographs of the wear tracks of flat surfaces lubricated under different oil types in this study are presented in Fig. 9. The flat surfaces of RSO and BRSO are

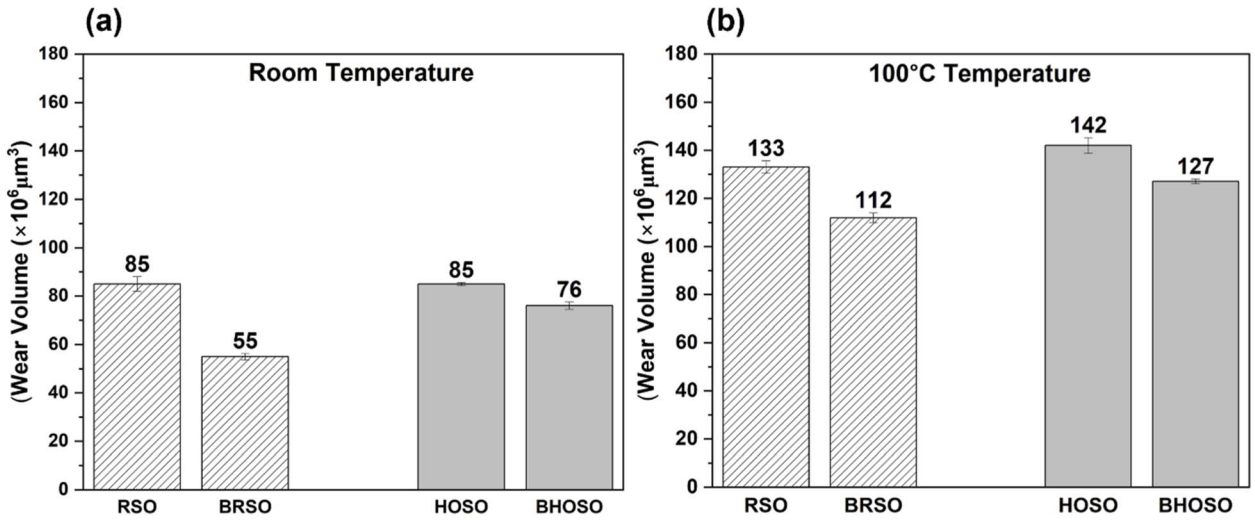

Fig. 7 Comparative wear volume analysis of flat samples (a) room temperature (b) 100 °C temperatures.

Table 2 Comparative fatty acid (monomeric) composition of various oils

	Palmitic acid	Stearic acid	Oleic acid	Linoleic acid	Linolenic acid	i-Pr branched stearic	i-Pr branched oleic	2xi-Pr branched stearic
RSO	10.7%	3.9%	20.7%	57.9%	6.8%	—	—	—
HOSO	4.7%	2.3%	89.3%	3.8%	—	—	—	—
BRSO	29.4%	9.2%	—	—	—	44.0%	2.9%	14.3%
BHOSO	6.3%	2.8%	2.5%	2.1%	—	86.3%	—	—

Table 3 Comparison of the physicochemical characteristics of the sample lubricants[a]

	Temperature (°C)	RSO	BRSO	HOSO	BHOSO
Density (g cm^{-3})	40	0.9066 ± 0.0	0.9242 ± 0.0	0.8993 ± 0.0	0.8965 ± 0.0
	100	0.8668 ± 0.0	0.8842 ± 0.0	0.8596 ± 0.0	0.8573 ± 0.0
Kinematic viscosity (mm^2 s^{-1})	40	30.69 ± 0.0	1283.0 ± 1.2	38.93 ± 0.01	142.13 ± 0.04
	100	7.53 ± 0.0	132.4 ± 1.3	8.49 ± 0.0	19.39 ± 0.02
Dynamic viscosity (mPa s^{-1})	40	27.82 ± 0.0	1185.7 ± 1.8	35.02 ± 0.01	127.42 ± 0.03
	100	6.52 ± 0.0	117.0 ± 1.4	7.30 ± 0.0	16.62 ± 0.01
Viscosity index		228.4 ± 0.1	210.8 ± 0.0	203.6 ± 0.04	155.9 ± 0.6
Oxidative onset temp, OT (°C)		175.7 ± 2.0	195.8 ± 1.5	202.2 ± 0.1	199.2 ± 0.6
Oxidative peak temp, PT (°C)		189.8 ± 1.8	217.6 ± 3.1	210.9 ± 1.4	213.7 ± 0.7
Pour point (PP, °C)		−15 ± 0.2	−12 ± 0.1	−15 ± 0.1	−12 ± 0.2
Cloud point (CP. °C)		−8.1 ± 0.2	−19.5 ± 0.3	−10.9 ± 0.2	−14.5 ± 0.2

[a] The average of each property is derived from three independent tests.

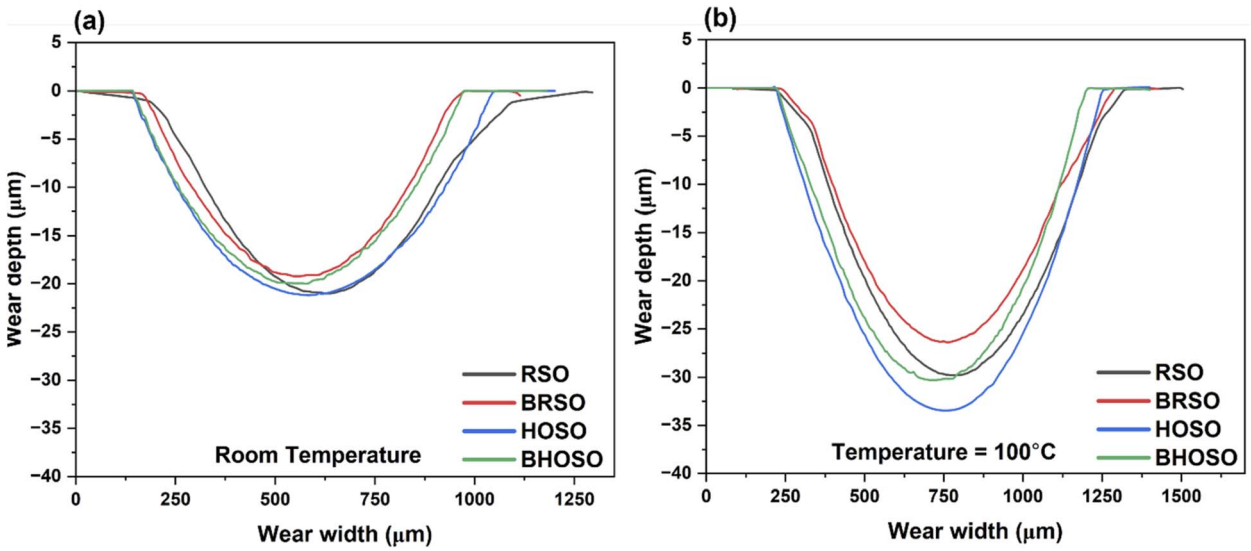

Fig. 8 Wear depth analysis of flat samples at (a) room temperature (b) 100 °C temperatures.

presented in Fig. 9a and b respectively. At room temperature, RSO exhibited removal of metal flakes or spalling, whereas BRSO did not. At high temperature, spalling or removal of material was observed in several positions for RSO, but only minor cracks were observed for BRSO. Furthermore, the wear width was reduced by approximately 14% for BRSO at both conditions, the wear width increased for both oils, with BHOSO having 5% less width than RSO. Furthermore, the wear width was reduced by approximately 14% at 40 °C and 6% at 100 °C for BRSO, whereas BHOSO showed only about a 4% reduction compared to HOSO under both conditions. The reduction in wear width helped to decrease the volume of wear for both conditions for BRSO.

The wear tracks of HOSO and BHOSO at both temperatures are presented in Fig. 9c and d, respectively. At room temperature, minor material dislodgement was observed throughout the HOSO track, while no major cracks or material removal were observed in BHOSO. However, at high temperatures, metal flaking was observed in both lubricants, while HOSO showed severe flaking in several places across the wear track and BHOSO exhibited in a few discrete regions. Despite this, the wear width was decreased by only 3.5% in both temperature conditions for HOSO, which helped to reduce the overall wear volume. The EDS analyses of the tests conducted at room temperature are presented in Fig. S2.† These analyses revealed the presence of Fe and Cr, which were inherent components of the flat samples. Furthermore, no Si from the balls was detected on the flat surface in the EDS analyses. The results for the high-temperature tests were similar. The results indicated that abrasive wear was the dominant mechanism in the flats for both temperature conditions, with no transfer of material observed. Abrasive wear occurs when abrasive particles or materials, which are harder than the surface being worn, cause material removal from one or both surfaces.

The wear tracks showed evidence of corrosion-induced pits. At room temperature, BRSO exhibited both pits and small cracks, which explains the reasons behind higher coefficient of friction (Fig. 9). Conversely, at high temperatures, there were

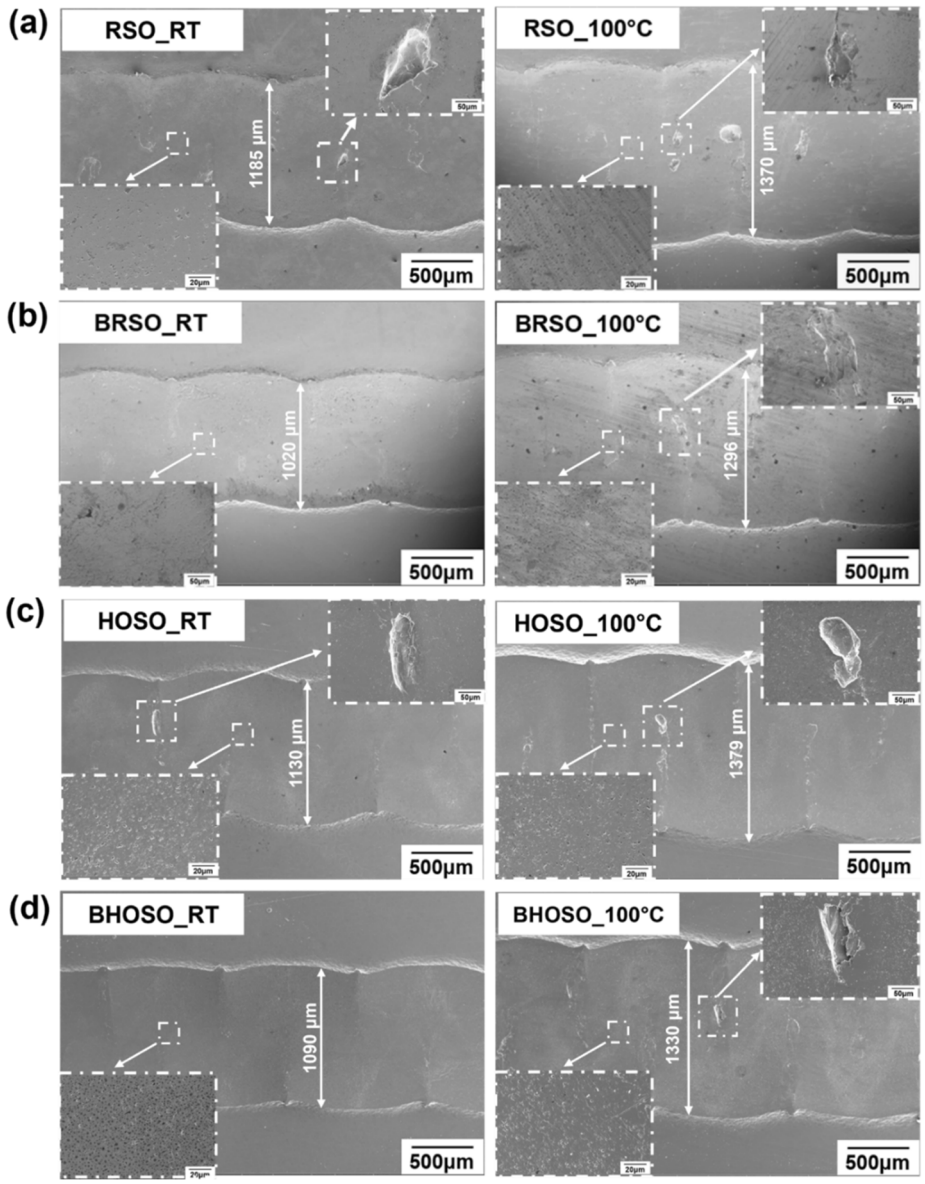

Fig. 9 SEM analysis of wear tracks on flat surfaces for (a) RSO, (b) BRSO, (c) HOSO, and (d) BHOSO at room temperature and 100 °C temperature.

fewer pits as compared to room temperature resulting in a lower coefficient of friction under those conditions.

4. Conclusion

The major findings from this systematic effort on isopropylation on regular and high oleic soybean oil are listed below:

• Regular and high oleic soybean oils were chemically modified by adding an isopropyl group at the double bond sites using ethylaluminum sesquichloride ($Et_3Al_2Cl_3$) catalyst. Physicochemical analysis showed that the introduction of an isopropyl group in BRSO slightly increased its density due to higher molecular weight and reduced *cis*-unsaturation. BRSO's viscosity at 40 °C was 42 times higher than RSO, and BHOSO was four times more viscous than HOSO, with viscosity decreasing exponentially with temperature. BRSO resulted in higher oxidation stability (OT and PT) due to fewer unsaturated bonds than RSO.

• HOSO presented the lowest coefficient of friction (COF) at both room and high temperatures, likely due to tocopherol. At room temperature, BHOSO showed a significant increase in friction, while RSO had a higher COF than HOSO. At 100 °C, COF decreased for all samples due to lower viscosity and increased lubricant mobility. The higher COF in modified oils (BHOSO, BRSO) was attributed to carbon branching, irregular shape, and higher viscosity.

• BRSO reduced wear volume more than BHOSO at both room temperature (35% *vs.* 10.5%) and 100 °C (15.7% *vs.* 10.5%), likely due to its higher palmitic acid (saturated fatty acid) and oligomer content. Wear resistance decreased at 100 °C due to material softening and reduced lubricant viscosity,

leading to less effective lubrication. Abrasive wear was the primary mechanism in all samples, with no material transfer from ball to flat samples. RSO showed spalling and cracks at both temperatures, while BRSO had only minor cracks at high temperature. HOSO and BHOSO exhibited minor material dislodgement at room temperature, but metal flaking was evident at high temperatures.

Overall, this investigation presents a holistic overview on the effect of a major chemical modification process on both regular and high oleic versions of soybean oils. The detailed friction and wear analyses along with wear mechanisms investigation for both room and high temperature can help decide lubricant experts and application engineers the base stock and chemical modification process wisely depending on the application requirements.

Data availability

The authors confirm that the data supporting the findings of this study are available within the article and its ESI.† Additional raw and/or derived data supporting the findings of this study can be available from the corresponding author (S. R.) on request.

Conflicts of interest

There are no conflicts to declare.

Acknowledgements

The authors express their gratitude to the North Dakota Soybean Council for generously providing the funding that supported the research endeavors. The authors would like to extend their sincere gratitude to Jay Evenstad from the University of North Dakota for his invaluable support in fabricating the sample holder for the tribological testing.

References

1 D. Tabor, Friction-The Present State of Our Understanding 1, *J. Tribol.*, 1981, **103**(2), 169–179.
2 R. Saidur, E. A. Abdelaziz, A. Demirbas, M. S. Hossain and S. Mekhilef, A review on biomass as a fuel for boilers, *Renewable Sustainable Energy Rev.*, 2011, **15**(5), 2262–2289, DOI: **10.1016/j.rser.2011.02.015**.
3 T. Mang and W. Dresel, *Lubricants and Lubrication*, Wiley-VCH, 2007.
4 R. Vazquez-Duhalt, Environmental Impact Of Used Motor Oil, *Sci. Total Environ.*, 1989, **79**(Issue 1), 1–23.
5 F. Ed Erique Haus, J. German and G.-A. Junter, Primary biodegradability of mineral base oils in relation to their chemical and physical characteristics, *Chemosphere*, 2001, **45**(6–7), 983–990.
6 M. P. Schneider, Plant-oil-based lubricants and hydraulic fluids, *J. Sci. Food Agric.*, 2006, **86**(12), 1769–1780, DOI: **10.1002/jsfa.2559**.
7 M. Höök and X. Tang, Depletion of fossil fuels and anthropogenic climate change-A review, *Energy Policy*, 2013, **52**, 797–809.
8 S. Roy, in *Multifunctional Bio-Based Lubricants: Synthesis, Properties and Applications*, 2023.
9 J. C. J. Bart, E. Gucciardi and S. Cavallaro, in *Biolubricants*, Elsevier, 2013, pp. 1–9.
10 C. J. Reeves and P. L. Menezes, Evaluation of boron nitride particles on the tribological performance of avocado and canola oil for energy conservation and sustainability, *Int. J. Adv. Manuf. Technol.*, 2017, **89**, 3475–3486.
11 A. Adhvaryu and S. Z. Erhan, Epoxidized soybean oil as a potential source of high-temperature lubricants, *Ind. Crops Prod.*, 2002, **15**(3), 247–254.
12 B. K. Sharma, J. M. Perez and S. Z. Erhan, Soybean oil-based lubricants: A search for synergistic antioxidants, *Energy Fuels*, 2007, **21**, 2408–2414.
13 P. Bhowmik, B. K. Sharma, M. I. Sarker, H. Choi, C. Tang and S. ROY, Investigating the impact of a newly developed chemical modification technique on improving the tribological properties of high oleic soybean oil, *Sustainable Energy Fuels*, 2024, **8**, 1314–1328, DOI: **10.1039/D3SE01526B**.
14 N. H. A. Ameen and E. Durak, Study of the tribological properties the mixture of soybean oil and used (waste) frying oil fatty acid methyl ester under boundary lubrication conditions, *Renewable Energy*, 2020, **145**, 1730–1747.
15 M. P. Schneider, Plant-oil-based lubricants and hydraulic fluids, *J. Sci. Food Agric.*, 2006, **86**(12), 1769–1780, DOI: **10.1002/jsfa.2559**.
16 J. Pichler, R. Maria Eder, L. Widder, M. Varga, M. Marchetti-Deschmann and M. Frauscher, Moving towards green lubrication: tribological behavior and chemical characterization of spent coffee grounds oil, *Green Chem. Lett. Rev.*, 2023, **16**(1), 2215243, DOI: **10.1080/17518253.2023.2215243**.
17 T. Unugul, T. Kutluk, B. Gürkaya Kutluk and N. Kapucu, Environmentally Friendly Processes from Coffee Wastes to Trimethylolpropane Esters to be Considered Biolubricants, *J. Air Waste Manage. Assoc.*, 2020, 1198–1215.
18 N. J. Fox, B. Tyrer and G. W. Stachowiak, Boundary lubrication performance of free fatty acids in sunflower oil, *Tribol. Lett.*, 2004, **16**, 275–281.
19 R. Kumar and R. K. Gautam, Tribological investigation of sunflower and soybean oil with metal oxide nanoadditives, *Biomass Convers. Biorefin.*, 2022, **14**, 2389–2401.
20 C. Zhao, Y. Jiao, Y. K. Chen and G. Ren, The Tribological Properties of Zinc Borate Ultrafine Powder as a Lubricant Additive in Sunflower Oil, *Tribol. Trans.*, 2014, **57**, 425–434.
21 B. Shomchoam and B. Yoosuk, Eco-friendly lubricant by partial hydrogenation of palm oil over Pd/γ-Al2O3 catalyst, *Ind. Crops Prod.*, 2014, **62**, 395–399.
22 H. H. Masjuki, M. A. Maleque, A. Kubo and T. Nonaka, Palm oil and mineral oil based lubricants-their tribological and emission performance, *Tribol. Lett.*, 1999, **32**(6), 305–314.

23 N. Sapawe, M. Farhan Hanafi and S. Samion, The Use of Palm Oil as New Alternative Biolubricant for Improving Anti-Friction and Anti-Wear Properties, *Mater. Today: Proc.*, 2019, **19**(Part 4), 1126–1135.

24 A. Ruggiero, R. D'Amato, M. Merola, P. Valašek and M. Müller, Tribological characterization of vegetal lubricants: Comparative experimental investigation on Jatropha curcas L. oil, Rapeseed Methyl Ester oil, Hydrotreated Rapeseed oil, *Tribol. Lett.*, 2017, **109**, 529–540.

25 N. Talib, R. M. Nasir and E. A. Rahim, Tribological behaviour of modified jatropha oil by mixing hexagonal boron nitride nanoparticles as a bio-based lubricant for machining processes, *J. Cleaner Prod.*, 2017, **147**, 360–378.

26 N. H. Jayadas, K. Prabhakaran Nair and A. G, Tribological evaluation of coconut oil as an environment-friendly lubricant, *Tribol. Lett.*, 2007, **40**, 350–354.

27 N. H. Jayadas and K. P. Nair, Coconut oil as base oil for industrial lubricants-evaluation and modification of thermal, oxidative and low temperature properties, *Tribol. Lett.*, 2006, **39**, 873–878.

28 C. P. Koshy, P. K. Rajendrakumar and M. V. Thottackkad, Evaluation of the tribological and thermo-physical properties of coconut oil added with MoS2 nanoparticles at elevated temperatures, *Wear*, 2015, **330–331**, 288–308.

29 J. Milano, A. H. Shamsuddin, A. S. Silitonga, A. H. Sebayang, M. A. Siregar, H. H. Masjuki, M. A. Pulungan, S. R. Chia and M. F. M. A. Zamri, Tribological study on the biodiesel produced from waste cooking oil, waste cooking oil blend with Calophyllum inophyllum and its diesel blends on lubricant oil, *Energy Rep.*, 2022, **8**, 1578–1590.

30 C. P. do Valle, J. S. Rodrigues, L. M. U. D. Fechine, A. P. Cunha, J. Queiroz Malveira, F. M. T. Luna and N. M. P. S. Ricardo, Chemical modification of Tilapia oil for biolubricant applications, *J. Cleaner Prod.*, 2018, **191**, 158–166.

31 B. Angulo, J. M. Fraile, L. Gil and C. I. Herrerías, Bio-lubricants production from fish oil residue by transesterification with trimethylolpropane, *J. Cleaner Prod.*, 2018, **202**, 81–87.

32 H. O. Yosief, M. I. Sarker, G. B. Bantchev, R. O. Dunn and S. C. Cermak, Chemical Modification of Beef Tallow for Lubricant Application, *Ind. Eng. Chem. Res.*, 2022, **61**, 9889–9900.

33 H. O. Yosief, M. I. Sarker, G. B. Bantchev, R. O. Dunn and S. C. Cermak, Physico-chemical and tribological properties of isopropyl-branched chicken fat, *Fuel*, 2022, **316**, 123293, DOI: **10.1016/j.fuel.2022.123293**.

34 K. Dziosa, Właściwości Smarne Oleju Z Alg W Skojarzeniu Stal-Stal Lubricating Properties Of Algae Oil In Steel-Steel Tribosystem, *Tribologia*, 2013, **251**(5), 21–31.

35 P. K. Mishra and S. Mukherji, Biosorption of diesel and lubricating oil on algal biomass, *3 Biotech*, 2012, **2**, 301–310.

36 F. M. T. Luna, J. B. Cavalcante, F. O. N. Silva and C. L. Cavalcante, Studies on biodegradability of bio-based lubricants, *Tribol. Lett.*, 2015, **92**, 301–306.

37 N. Salih and J. Salimon, A Review on Eco-Friendly Green Biolubricants from Renewable and Sustainable Plant Oil Sources, *Biointerface Res. Appl. Chem.*, 2021, **11**, 13303–13327.

38 S. Shrivastava, P. Prajapati, Virendra, P. Srivastava, A. P. S. Lodhi, D. Kumar, V. Sharma, S. K. Srivastava and D. D. Agarwal, Chemical transesterification of soybean oil as a feedstock for stable biodiesel and biolubricant production by using Zn Al hydrotalcites as a catalyst and perform tribological assessment, *Ind. Crops Prod.*, 2023, **192**, 116002, DOI: **10.1016/j.indcrop.2022.116002**.

39 H. S. Hwang and S. Z. Erhan, Synthetic lubricant basestocks from epoxidized soybean oil and Guerbet alcohols, *Ind. Crops Prod.*, 2006, **23**, 311–317.

40 N. A. Fathurrahman, A. S. Auzani, R. Zaelani, R. Anggarani, L. Aisyah, Maymuchar and C. S. Wibowo, Lubricity Properties of Palm Oil Biodiesel Blends with Petroleum Diesel and Hydrogenated Vegetable Oil, *Lubricants*, 2023, **11**(4), 176, DOI: **10.3390/lubricants11040176**.

41 H. O. Yosief, M. I. Sarker, G. B. Bantchev and R. O. Dunn, Isopropyl-branched lard and its potential application as a bio-based lubricant, *Lubr. Sci.*, 2023, **36**(2), 104–118, DOI: **10.1002/ls.1673**.

42 H. K. D. H. Bhadeshia, Steels for bearings, *Prog. Mater. Sci.*, 2012, **57**(2), 268–435, DOI: **10.1016/j.pmatsci.2011.06.002**.

43 R. T. Cundill, High precision silicon nitride balls for bearings, *Proc. SPIE 1573, Commercial Applications of Precision Manufacturing at the Sub-Micron Level*, 1992, vol. 1573.

44 F. He, G. Xie and J. Luo, *Electrical Bearing Failures in Electric Vehicles*, Tsinghua University Press, 2020, vol. 8, pp. 4–28, DOI: **10.1007/s40544-019-0356-5**.

45 R. Raga, I. Khader, Z. Chlup and A. Kailer, Damage initiation and evolution in silicon nitride under non-conforming lubricated hybrid rolling contact, *Wear*, 2016, **360–361**, 147–159.

46 V. Brizmer, A. Gabelli, C. Vieillard and G. E. Morales-Espejel, An Experimental and Theoretical Study of Hybrid Bearing Micropitting Performance under Reduced Lubrication, *Tribol. Trans.*, 2015, **58**, 829–835.

47 ASTM International, Standard Test Method for Dynamic Viscosity and Density of Liquids by Stabinger Viscometer (and the Calculation of Kinematic Viscosity) 1, ASTM International, 2014, DOI: **10.1520/D7042-21**.

48 ASTM International, Standard Test Method for Density, Relative Density, and API Gravity of Liquids by Digital Density Meter 1, ASTM International, Last Updated: May 18, 2022, DOI: **10.1520/D4052-18A**.

49 ASTM International, Standard Practice for Calculating Viscosity Index from Kinematic Viscosity at 40 °C and 100 °C 1, ASTM International, Last Updated: May 13, 2024, DOI: **10.1520/D2270-10R16**.

50 ASTM International, Standard Test Method for Cloud Point of Petroleum Products and Liquid Fuels (Constant Cooling Rate Method) 1, ASTM International, Last Updated: Jan 27, 2021, DOI: **10.1520/D5773-21**.

51 ASTM International, Standard Test Method for Pour Point of Petroleum Products (Automatic Pressure Pulsing Method) 1,

ASTM International, Last Updated: Aug 12, 2022, DOI: 10.1520/D5949-16R22.

52 C. J. Ifedi, *A High Torque Density, Direct Drive In-Wheel Motor for Electric Vehicles*, Newcastle University, 2013.

53 B. Zhmud, M. Najjari and B. Brodmann, The Effects of the Lubricant Properties and Surface Finish Characteristics on the Tribology of High-Speed Gears for EV Transmissions, *Lubricants*, 2024, **12**(4), 112, DOI: 10.3390/lubricants12040112.

54 S. N. Sahasrabudhe, V. Rodriguez-Martinez, M. O'Meara and B. E. Farkas, Density, viscosity, and surface tension of five vegetable oils at elevated temperatures: Measurement and modeling, *Int. J. Food Prop.*, 2017, **20**, 1965–1981.

55 A. Martini, U. S. Ramasamy and M. Len, Review of Viscosity Modifier Lubricant Additives, *Tribol. Lett.*, 2018, **66**, 58, DOI: 10.1007/s11249-018-1007-0.

56 E. G. Giakoumis and C. K. Sarakatsanis, Estimation of biodiesel cetane number, density, kinematic viscosity and heating values from its fatty acid weight composition, *Fuel*, 2018, **222**, 574–585.

57 I. K. Hong, G. S. Jeon and S. B. Lee, Prediction of biodiesel fuel properties from fatty acid alkyl ester, *J. Ind. Eng. Chem.*, 2014, **20**, 2348–2353.

58 G. E. Napolitano, Y. Ye and C. Cruz-Hernandez, Chemical Characterization of a High-Oleic Soybean Oil, *J. Am. Oil Chem.' Soc.*, 2018, **95**, 583–589.

59 C. M. Seppanen, Q. Song and A. Saari Csallany, The antioxidant functions of tocopherol and tocotrienol homologues in oils, fats, and food systems, *J. Am. Oil Chem. Soc.*, 2010, **87**, 469–481, DOI: 10.1007/s11746-009-1526-9.

60 S. Roy, B. C. Stump, H. Luo, D. Leonard and J. Qu, Why does a phosphonium-phosphinate ionic liquid protect the contact surfaces from wear and micropitting but increase vibration when used as an additive in rolling-sliding lubrication?, *Tribol. Lett.*, 2021, **159**, 106949, DOI: 10.1016/j.triboint.2021.106949.

61 S. Roy, L. Speed, M. Viola, H. Luo, D. Leonard and J. Qu, Oil miscible phosphonium-phosphate ionic liquid as novel antiwear and antipitting additive for low-viscosity rear axle lubricants, *Wear*, 2021, **466–467**, 203588, DOI: 10.1016/j.wear.2020.203588.

62 N. K. Attia, S. A. El-Mekkawi, O. A. Elardy and E. A. Abdelkader, Chemical and rheological assessment of produced biolubricants from different vegetable oils, *Fuel*, 2020, **271**, 117578, DOI: 10.1016/j.fuel.2020.117578.

63 L. Wang and X. Liu, Tribological behavior of DLC/IL solid-liquid lubricating coatings in a high-vacuum condition with alternating high and low temperatures, *Wear*, 2013, **304**, 13–19.

64 J. Zhang, A. Tan and H. Spikes, Effect of Base Oil Structure on Elastohydrodynamic Friction, *Tribol. Lett.*, 2017, **65**, 13, DOI: 10.1007/s11249-016-0791-7.

65 K.-H. Hentschel Bayer, The Influence of Molecular Structure on the Frictional Behaviour of Lubricating Fluids, *J. Synth. Lubr.*, 1985, **2**(2), 143–165.

66 W. Hirst and A. J. Moore, Elastohydrodynamic Lubrication At High Pressures – 2. non-newtonian behavior, *Proc. R. Soc. London, Ser. A*, 1979, **365**, 537–565.

67 M. Muraki, Molecular structure of synthetic hydrocarbon oils and their rheological properties governing traction characteristics, *Tribol. Lett.*, 1987, **20**(Issue 6), 347–354.